Solvent and Structural Effects on Ultrafast Chelation Dynamics of Arene Chromium Tricarbonyl Sulfide Derivatives

Tung T. To† **and Edwin J. Heilweil***

Optical Technology Division, National Institute of Standards and Technology, Gaithersburg, Maryland 20899-8443

Charles B. Duke III and Theodore J. Burkey

Department of Chemistry, Campus Box 526060, University of Memphis, Memphis, Tennessee 38152-6060

Received: February 11, 2007; In Final Form: May 18, 2007

The chelation dynamics of three new $[Cr\{\eta^6\text{-}C_6H_5C(O)R\}(CO)_3]$ complexes, **1** [R = $CH_2(SCH_3)$], **2** [R = $CH(SCH_3)_2$], and **3** [R = $C(SCH_3)_3$], has been investigated on the picosecond to millisecond time scales by UV pump/IR probe transient absorption spectroscopy following photodissociation of CO in room temperature *n*-heptane, tetrahydrofuran (THF), and acetonitrile. In *n*-heptane, UV irradiation of **1**, **2**, or **3** dissociates CO to initially yield a Cr−S chelate (in which the pendant sulfide moiety is coordinated to the metal center) and a transient Cr−heptane solvate in approximately 1:2, 1:2, and 2:1 ratios, respectively. The Cr−heptane solvate is unstable and converts to the Cr−S chelate within 30 ns in each case. Irradiation of **2** or **3** in THF yields both the Cr−S chelate and Cr−THF solvate in approximately 1:3 and 1:1 ratios, respectively. The Cr−THF solvate converts to the Cr−S chelate on the second or longer time scale. All three complexes appear to yield the $Cr-NCCH_3$ solvate exclusively within 50 ps following irradiation in acetonitrile. The solvent effect on chelation is in striking contrast to that previously reported for the analogous $RCpMn(CO)_3$ derivatives, **4**−**6**. In acetonitrile, only chelation is observed for the Mn series and only solvent coordination is observed for the Cr series, but in heptane both chelation and solvent coordination are observed in both series.

Introduction

Reversible molecular photoswitches have potential applications as recordable media and reversible optical switches,[1] with high quantum yields, rapid response rates, and low fatigue being desirable properties of molecular photoswitches. We recently reported bistable, photochromic organometallics based on a linkage isomerization of complexes with a bifunctional, nonchelating ligand[2] and intramolecular ligand exchange of organometallic chelates with tethered functional groups.[3] In an effort to learn how to control and optimize these properties during the linkage isomerization of organometallic chelates, we previously investigated several model organometallic compounds capable of chelation following CO photodissociation. Certain chelatable functional groups in model compounds resulted in unit quantum yields for ligand substitution where simple bimolecular substitution never exceeds 0.8.[4] It is significant to note that a unit quantum yield indicates that there can be no CO recombination. If chelation competes with geminate CO recombination,[5] which can occur within 300 fs,[6] then the chelation must be ultrafast. Our studies indicate that the structure of the chelatable functional groups and solvent can greatly influence the quantum yield, reaction rate, and chelation pathways of organometallic complexes.[7] UV pump/IR probe transient picosecond to microsecond infrared experiments of manganese compounds **4**−**6** (Chart 1) in *n*-heptane show that UV irradiation induces ultrafast CO loss to eventually yield the stable Mn−S chelate in which the pendant sulfide moiety is coordinated with the unsaturated manganese metal center.[7b] This chelation process can occur via two pathways: a direct subpicosecond chelation pathway and a slower (greater than a nanosecond) solvent coordination pathway (Scheme 1). It appears that the fast chelation pathway depends on the close proximity of a sulfide group to the metal center to intercept the metal, before solvent coordination occurs. Conformation calculations suggest that the sulfide group(s) in **4** and **5** spend at least half of the time away from the metal center, whereas there is always a sulfide group near the metal center in **6**.[4,7b] Thus, only **6** undergoes chelation to the complete exclusion of solvent coordination upon UV irradiation in alkane solution. In contrast, all three manganese complexes follow a direct chelation pathway

CHART 1

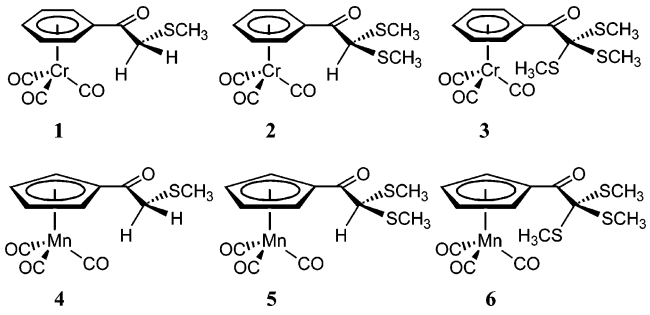

SCHEME 1

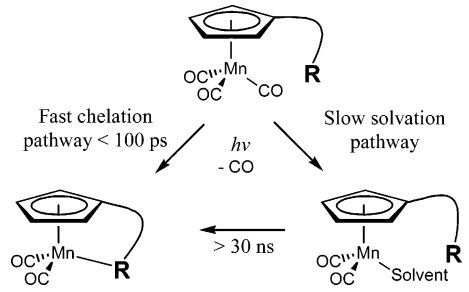

* Corresponding author. E-mail: edwin.heilweil@nist.gov.
† NIST Guest Researcher/Postdoctoral Associate.

10.1021/jp071172m CCC: $37.00
Published on Web 07/12/2007

upon UV irradiation without measurable solvation in acetonitrile,[7a] in spite of the fact that related Mn-acetonitrile adducts are stable.[2] Apparently, solvent effects position the sulfide group(s) in **4** and **5** near the metal center, thus allowing the Mn−S chelate to form before the unsaturated metal encounters acetonitrile.

To understand how the metal center and the structure of the chelating ligand may affect chelation rates and pathways, we prepared three new derivatives of the Cr species, **1**, **2**, and **3**, bearing identical sulfide side chains as the analogous Mn species, **4**, **5**, and **6**, respectively (Chart 1). In this report, we describe the photoinduced dynamics of **1**−**3** in three solvents, *n*-heptane, tetrahydrofuran (THF), and acetonitrile, and compare them to our earlier studies of **4**−**6**.

Experimental Section

A detailed description of the time-resolved UV pump/infrared probe (TRIR) apparatus used for this study was previously reported.[7] In a typical experiment with picosecond time resolution, a 289 nm UV pulse (ca. 120 fs pulse duration with 4−6 μJ energy) was focused to approximately 100 μm diameter in a 2 mm path length flow cell with CaF_2 windows. For nanosecond to millisecond resolution, 355 nm harmonic pulses from a Q-switched Nd:YAG laser (4 ns pulse duration, 30−40 μJ energy) were electronically synchronized and timed to the femtosecond IR probe pulses. We averaged 2000 laser shots to obtain a single difference spectrum. Two to four of these spectra were averaged for each time delay presented. Analysis of averaged spectra (typically four) yielded an intensity uncertainty from the baseline of less than ±0.005 optical density (OD) units ($k = 1$; type B analysis).

To prepare samples for the TRIR experiments, the Cr complexes (30−50 mg) were dissolved in 50−80 mL of solvent to produce millimolar concentrations (e.g., 1.2×10^{-3} mol/L from 30 mg of **1** in 80 mL of *n*-heptane) with optical density (OD) ∼1 measured at the higher CO-stretching frequency (e.g., near 1990 cm^{-1} in heptane) of the two Cr−CO stretching bands. All samples were studied at room temperature (ca. 293 K).

Preparation of 1−3. Previously reported syntheses of **5** and **6**[7] and 2,2-bis(methylthio)-1-phenylethanone and 2,2,2-tris(methylthio)-1-phenylethanone[8] were modified to produce **1**−**3**. Tris(methylthio)methane (2.9 mL, 22 mmol) in 40 mL of THF (tetrahydrofuran) was added to BuLi (12.5, 25 mmol, 2 M in pentane) and stirred at 195 K for 2 h. Methyl benzoate chromium tricarbonyl (2.0 g, 7.3 mmol) in 10 mL of THF was added, and the solution was allowed to warm to room temperature overnight. Upon quenching with water, extraction of the aqueous phase with ether, and concentration of the organic phase, the product was eluted with hexane/ethyl acetate on silica gel, yielding 93 mg (6.4%) of red powder **1**.[9] Similar procedures were used to produce 0.8 g (62%) of red crystalline **2** from tris(methylthio)methane (1.0 mL, 7.2 mmol) in 5 mL of THF, BuLi (4.0 mL, 8.0 mmol, 2 M in pentane) (stirred at 175 K), and methyl benzoate chromium tricarbonyl (1.0 g, 3.7 mmol) in 10 mL THF.[10] To prepare **3**, tris(methylthio)methane (0.7 mL, 5.0 mmol) in 10 mL of THF and BuLi (2.3 mL, 4.5 mmol, 2 M in pentane) were stirred at 175 K for 2 h. Methyl benzoate chromium tricarbonyl (2.7 g, 10.0 mmol) in 25 mL of THF was added.[11] After stirring at 175 K for 4 h, the resulting solution was quenched with water, the aqueous phase was extracted with ether, and the organic phase was concentrated by evaporation overnight, yielding 1.0 g (53%) of red crystalline **3**.

Acetonitrile (anhydrous), tris(methylthio)methane, butyllithium (BuLi), methyl benzoate, THF (anhydrous), and tris(methyl)thiomethane were obtained from Sigma-Aldrich Chemicals; *n*-heptane (analytical grade) was from the Mallinckrodt Chemicals, and $Cr(CO)_6$ was from Strem Chemical, and they were used without further purification.[12] Methyl benzoate chromium tricarbonyl was synthesized from methyl benzoate and $Cr(CO)_6$ according to literature procedures.[13]

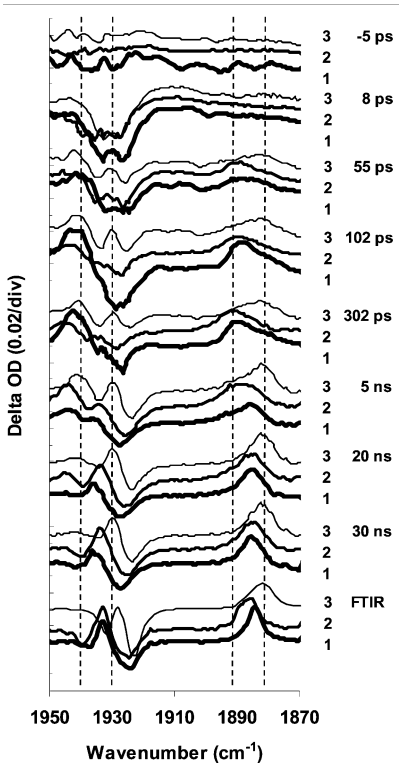

Figure 1. Transient TRIR difference spectra acquired after UV irradiation of **1**−**3** in *n*-heptane at 298 K. Presented within each labeled time delay, the thickest, medium, and thinnest spectral lines correspond to spectral changes of **1**, **2**, and **3**, respectively. At each time delay, the spectra are offset vertically by 0.01 OD units for clarity. At the bottom are the difference FTIR spectra of **1**−**3** (amplitude divided by a factor of 3) in *n*-heptane acquired before and after irradiation with a xenon arc lamp. Vertical dashed lines are aids for distinguishing transient Cr−heptane versus Cr−S dicarbonyl absorption features for **3** described in the text.

Results and Discussion

TRIR experiments performed in this work show that irradiation of **1**, **2**, or **3** in *n*-heptane solution at either 289 or 355 nm results in CO dissociation to initially form two photoproducts: the transient Cr−heptane solvate and stable Cr−S bound chelate. The Cr−heptane solvate eventually converts to the Cr−S chelate on the nanosecond time scale. Upon examining the difference TRIR spectral changes of **1** in Figure 1, strong bleaching signals from the starting compound's CO-stretching band doublet near 1926 and 1932 cm^{-1} are clearly observed at 8 ps time delay, indicating efficient photoexcitation and CO loss. A third bleach signal for the parent compound's highest frequency CO stretch occurs at 1990 cm^{-1} but is not examined in this study. A broad red-shifted absorption feature (relative to the doublet bleach feature) is observed around 1915 cm^{-1} that has been interpreted previously as arising from cooling of vibrationally hot species.[7b]

At the intermediate time delay of 102 ps, two absorption bands are observed near 1888 and 1940 cm^{-1}. These two absorptions decrease in intensity as the time delay increases and eventually disappear together at 30 ns. As the two features near 1888 and 1940 cm^{-1} decay in intensity, we note that the absorption intensity near 1880 cm^{-1} increases to generate a newly observed feature on the nanosecond time scale. Coincident with the growth of absorption intensity at 1880 cm^{-1}, another new absorption feature centered near 1934 cm^{-1} also

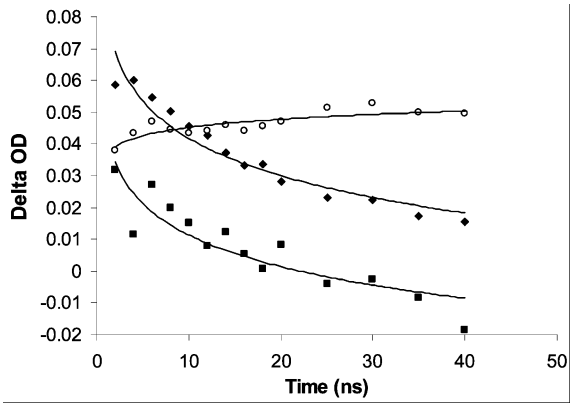

Figure 2. Representative nanosecond kinetics showing the decrease of the transient Cr-solvated absorption bands at 1942 cm^{-1} (solid squares) and 1890 cm^{-1} (solid diamonds) as the Cr−S chelate band at 1884 cm^{-1} (open circles) grows in absorption upon UV irradiation of **2** in heptane.

SCHEME 2

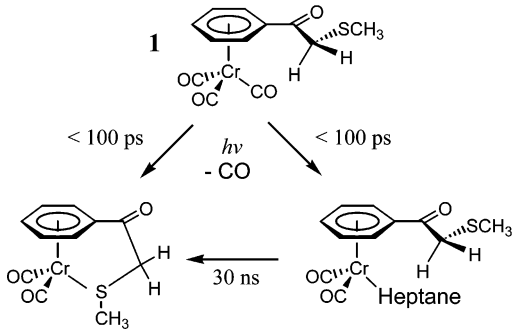

emerges on top of the parent bleach feature. These results indicate that there are two new dicarbonyl species initially formed upon UV irradiation of **1**, **2**, or **3** in *n*-heptane, and while one pair of CO bands disappears, the other pair grows, suggesting they are kinetically coupled. We assign the blue-shifted pair of CO stretching bands near 1888 and 1940 cm^{-1} to the Cr solvate and the red-shifted pair of CO stretching bands near 1880 and 1934 cm^{-1} (identical to that observed in the difference FTIR at the bottom of Figure 1) to the Cr−S chelate. The overall chelation reaction mechanism is summarized in Scheme 2, and representative kinetic traces highlighting the conversion of the Cr solvate to Cr−S chelate are shown in Figure 2. These assignments are also consistent with previously obtained results from transient and steady-state IR studies of **4**−**6** in *n*-heptane, in which the metal−heptane solvate intermediate has CO stretching bands blue-shifted relative to the CO stretching bands of the metal−S chelate.[4,7b] Additional support for these spectral assignments is derived from previously reported observations that (arene)$Cr(CO)_2$−alkane complexes are observed with up to microsecond lifetimes.[14] While it might be tempting to assign dynamic changes observed prior to 100 ps to interchange between the chelate and solvate, their rates of vibrational cooling may be different and therefore complicate such assignments.[15,16] There were no spectral changes between 100 and 300 ps, indicating that vibrational relaxation was complete.

The difference TRIR spectral changes observed for **2** and **3** in heptane (see Figure 1) are similar to those of **1**. However, having additional sulfide groups on the pendant side chain appears to diminish the competing solvent coordination. Apparently solvent coordination is not completely excluded for **3**, as was previously observed for the Mn analog (**6**).[7b] Examining the two overlapping absorption bands of **1** near 1880 and 1888 cm^{-1} at 102 ps time delay, we note that the absorption intensity at 1880 cm^{-1} of the Cr−S chelate is approximately half the absorption intensity at 1888 cm^{-1} arising from the Cr−heptane solvate. Assuming the Cr−S chelate and the Cr−heptane solvate have similar IR absorption cross sections, this result suggests that the initial Cr−S chelate/Cr−heptane solvate ratio is approximately 1:2. Applying the same analysis to the other Cr−S species, the initial Cr−S chelate/Cr−heptane solvate distribution is slightly larger than 1:2 upon the irradiation of **2** and ∼2:1 upon the irradiation of **3**.

Previous conformational analyses of the manganese analogs **4**−**6** showed that the most energetically favorable conformations of the manganese complexes position the side chain carbonyl group in the Cp plane (Cp = cyclopentadienyl).[4,7b] As a result, the sulfide group in **4** is near the Mn metal center 50% of the time, while all lowest energy conformations of **6** position a sulfide group near the Mn metal center all the time. Hence, the chelate:solvate population distribution immediately after photolysis of **4** and **5** is approximately 1:1, and there is no solvate observed after irradiation of **6** in *n*-heptane solution. If the initial product distribution depends on the side chain availability and the unsaturated metal center reacts with the first species it encounters,[4] then the sulfide group(s) in **1** and **2** should be near the metal center at least ∼33% of the time, while a sulfide group for **3** would be near the metal center ∼66% of the time to produce the above observed initial product distribution. This argument implies that conformational or other structural features position pendant sulfides better for reaction for the CpMn derivatives than the benzene−Cr derivatives. For example, the potential well for rotation of the side chain carbonyl group relative to the arene ring may be deeper and therefore "narrower" for **4**−**6** compared to **1**−**3**, forcing sulfide groups of **4**−**6** to generally spend more time near the metal. A more plausible explanation may be that the larger benzene ring holds the sulfide groups farther away from the metal center than the cyclopentadienyl ring. The lowest energy conformations determined by density functional theory (DFT isolated molecule calculations using Gaussian 03 software with B3LYP/6-31G$^+$ for method/basis set) indicate that the nearest neighbor sulfur is 0.2 Å further away from the Cr compared to Mn. Finally DFT calculations reveal a higher charge on Mn (+2.1) versus Cr (+0.6), resulting in a greater attraction of the polar sulfide groups in the Mn complexes, which may make chelation more probable.

Figure 3 shows transient difference spectra of **2** and **3** in THF solution recorded at pump−probe delay times ranging from picoseconds to milliseconds and FTIR difference spectra of **1**−**3** and **7** (Scheme 3) before and after 30 s of UV irradiation with a xenon arc lamp (the FTIR spectral acquisition time was approximately 1 min). Since **7** has no chelatable side chain, we conclude that irradiation of **7** in THF yields the Cr−THF adduct, **8**, having characteristic IR bands at 1842 and 1906 cm^{-1}. These same absorption bands, also observed in the difference TRIR experiments, are therefore assigned to the Cr−THF solvate. Apparently, the chelation dynamics of **1**−**3** in THF are similar to that observed in *n*-heptane, with the exception that the dominant chelation pathway in THF is via the Cr−THF solvate. It is more difficult to obtain good signals in THF because, unlike *n*-heptane, THF strongly absorbs in the IR region of the photoproducts. Difference absorption signals for picosecond time scale studies are slightly weaker than for the nanosecond time scale, due to much lower available UV pump pulse power for the picosecond investigations. We did not study the chelation of **1** on the picosecond time scale because the results obtained from nanosecond experiments and studies in *n*-heptane suggested that there would be no significant difference in the chelation dynamics between **1** and **2**. In any event, broad absorptions [ca. 30 cm^{-1} full-width at half-maximum (fwhm)] near 1842 cm^{-1} from **1** and **2** and 1858 cm^{-1} from **3** are

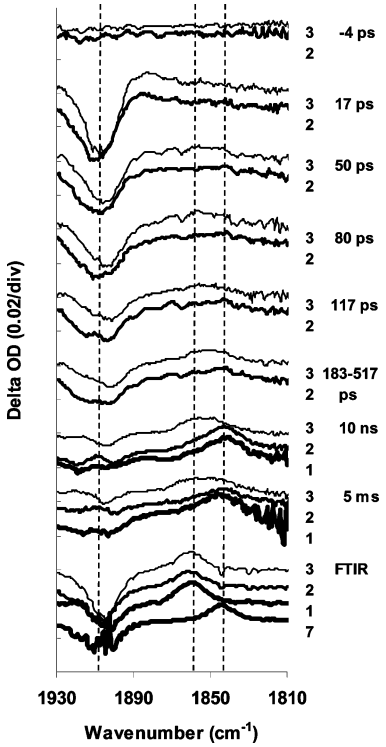

Figure 3. Transient TRIR difference spectra acquired after UV irradiation of **1**−**3** in THF at 298 K. **1** was not investigated for picosecond delay times because it showed similar dynamics to **2** in *n*-heptane (see Figure 1). At each time delay, the spectra are offset vertically by 0.01 OD units for clarity. At the bottom are difference FTIR spectra of **1**, **2**, **3**, and **7** (amplitude divided by a factor of 2) in THF acquired before and after irradiation with a xenon arc lamp. Vertical dashed lines are aids to distinguish overlapping absorption features from Cr−solvate vs Cr−S species.

SCHEME 3

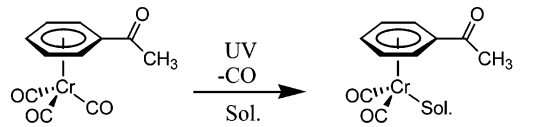

7

8 Sol. = THF
9 Sol. = $NCCH_3$

observed, particularly in the nanosecond regime, which remained unchanged up to microsecond time delays (not shown). The fact that the fwhm of these features is ca. 1.5 times broader than all other bands observed in the difference FTIR spectra and that their base widths extend beyond the overlaying absorptions of the chelate and the solvate as observed in the difference FTIR spectra imply they are composed of more than one CO stretching band. Using the difference TRIR spectra at 10 ns, where the best signal-to-noise ratio for all three complexes was obtained, we note that the absorption intensity at 1858 cm^{-1} is approximately 0.33 the absorption intensity at 1842 cm^{-1} from the irradiation of **1** and **2**, but both of the intensities are the same from irradiation of **3**. In addition, simulated spectra 1a, 2a, and 3a (see Figure 4), in which the steady-state FTIR difference spectra of **1**, **2**, or **3** in THF are linearly combined with that of **7** as 1a = (**1**)/3 + 1 × (**7**), 2a = (**2**)/3 + 1 × (**7**), and 3a = 1 × (**3**) +1 × (**7**), produces nearly identical spectral features obtained from the transient TRIR experiments of **1**, **2**, and **3** in THF. Two additional transient bands near 1906 and 1918 cm^{-1} are largely obscured by the parent species bleach band at 1906 cm^{-1}. Our TRIR spectrometer can monitor spectral changes up to 5 ms; however, the FTIR difference spectra show that the final products of **1**−**3** are not the Cr−THF solvates but

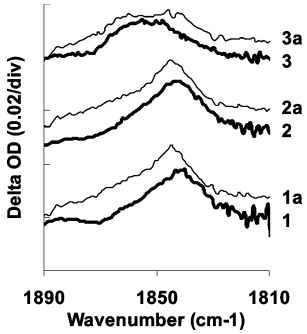

Figure 4. Simulated steady-state spectra (thin lines 1a, 2a, and 3a), in which the steady-state FTIR difference spectral bands of **1**, **2**, and **3** in THF are combined in the following way: 1a = (**1**)/3 + 1 × (**7**); 2a = (**2**)/3 + 1 × (**7**); and 3a = 1 × (**3**) +1 × (**7**). The simulation produces nearly identical spectral features to those observed in the 10 ns transient TRIR experiments for **1**−**3** in THF (thick lines).

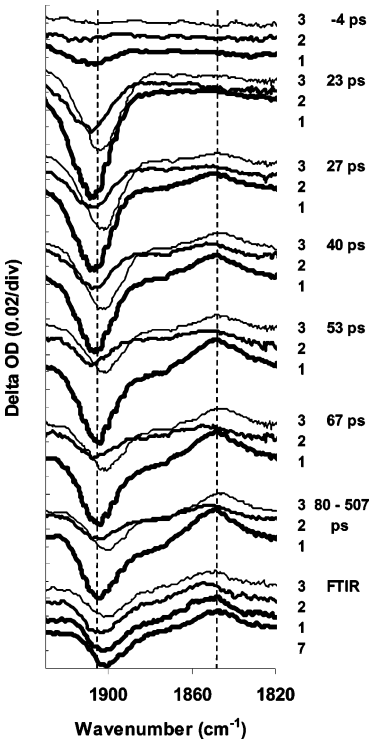

Figure 5. TRIR difference spectra acquired after UV irradiation of **1**−**3** in acetonitrile at 298 K. The spectra are offset vertically by 0.01 OD units for clarity. At the bottom are difference FTIR spectra of **1**−**3** and **7** (amplitude divided by a factor of 2) in acetonitrile acquired before and after irradiation with a xenon arc lamp.

the Cr−S chelates. The combined results from the TRIR and steady-state FTIR experiments indicate that the solvate Cr−THF species eventually converts to the Cr−S chelate on a time scale greater than 5 ms. These results indicate that (1) the ultrafast coordination of solvent is more favorable for the stronger coordinating solvent and therefore chelation in THF occurs mainly via the Cr solvate and (2) the stronger the Cr−solvent bond, the longer time it takes for the Cr solvate to convert to the Cr−S chelate.

Figure 5 shows transient difference spectra for **1**−**3** in acetonitrile recorded at pump−probe delay times ranging from −4 to 80 ps. Unlike the results obtained from irradiation of **1**−**3** in *n*-heptane and THF, the spectral changes observed for all three complexes in acetonitrile are nearly identical. A bleach band from the starting compound is clearly observed at 1905 cm^{-1} (the second high-frequency bleach band occurs at 1977

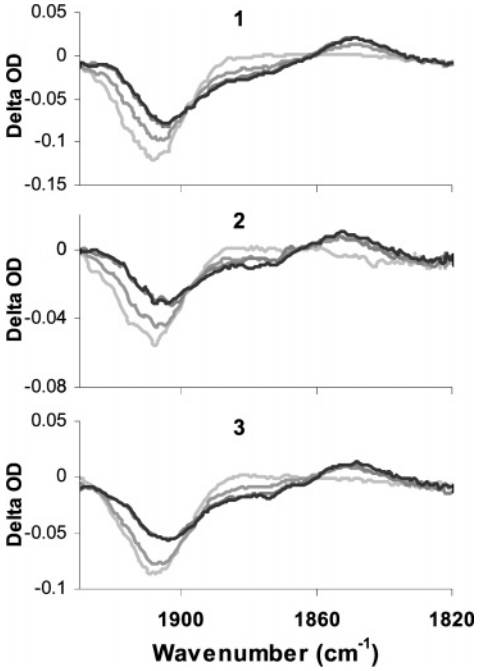

Figure 6. Overlapped transient TRIR difference spectra from Figure 5 of **1**−**3** in acetonitrile at 298 K highlighting two isosbestic points at 1895 and 1860 cm^{-1}. The lightest and darkest spectra were obtained at 13 and 107 ps time delays, respectively. The two intermediate time-delayed spectra were obtained at 40 and 90 ps, where the 40 ps spectrum has the second strongest bleach intensity near 1905 cm^{-1}.

cm^{-1} and was not examined). For delay times greater than 23 ps, a broad absorption band (ca. 20 cm^{-1} fwhm) appears at 1846 cm^{-1}. When the transient spectra are overlapped between 13 and 107 ps (see Figure 6), we observe isosbestic points near 1895 and 1860 cm^{-1}, which indicates a clean conversion from the parent tricarbonyl molecule to a photoproduct. The transient difference spectra after 27 ps are nearly identical to those obtained from the steady-state experiments (bottom of Figure 5). The acetophenone chromium tricarbonyl complex **7** has similar ground-state CO stretch absorption bands (appear as bleaches in the difference FTIR spectra) as those of **1**−**3**, and the FTIR difference spectrum obtained by steady-state irradiation of **7** producing **9** (Scheme 3) in acetonitrile results in nearly identical TRIR difference spectra of **1**−**3** in acetonitrile. Despite many attempts to prepare Cr−S chelates in acetonitrile, they could not be isolated or observed, whereas stable isolated chromium acetonitrile complexes are known.[17] In pure solvent with no diffusion, and assuming minimal entropic effects, these results suggest that the bond energies of the Cr−S chelate and the Cr−solvate are most likely in the order Cr−heptane < Cr−THF < Cr−S (chelate) ≤ Cr−acetonitrile. If the initial product distribution upon irradiation of **1**−**3** is determined not only by the accessibility of the sulfide group but also by the coordination power (as was observed from the TRIR experiments in *n*-heptane and THF), then the transient TRIR experimental results suggest that irradiation of **1**−**3** in acetonitrile yields the Cr−$NCCH_3$ solvate, with no evidence for sulfur chelation.

Conclusions

The results from this investigation indicate that the reaction rates and chelation pathways of the chromium series (**1**−**3**) complexes depend on the conformational accessibility of the chelatable side group. These substitution reactions are influenced by the structure of the side chain, the metal center, and the coordination power of the solvent. We found that there is competition between immediate chelation and solvent coordination following CO dissociation of **1**, **2**, or **3** in *n*-heptane and THF solutions to form two initial products: Cr−S chelate and Cr−Sol solvate (Sol = *n*-heptane or THF), which is a similar pattern observed for the analogous manganese compounds (**4**−**6**). The picosecond dynamics is governed by side chain availability versus solvent strength, which determines the relative contribution of transient solvate versus chelate populations. The interconversion of solvate to chelate occurs on the nansecond to much longer time scale, depending on the Cr−solvent bond strength. This study highlights how subtle structural changes may be used to tailor picosecond processes for the design of ultrafast molecular switches. More extensive studies are underway where the multiplicity of the electronic state will be considered.

Acknowledgment. This work was partly supported by the National Science Foundation under Grant No. CHE-0227475 (T.J.B.) and internal NIST Scientific, Technical, and Research Services funding (C.B.D., T.T.T., and E.J.H.). We also thank Dr. Okan Essenturk (U. Maryland NIST Guest Researcher) for his valuable discussions and help with molecular structure DFT calculations.

References and Notes

(1) (a) For leading references on photochromic materials in photonic devices, see: Irie, M. Ed. *Chem. Rev.* **2000**, *100*, 1683. (b) For a recent review on the use of photochromic materials for optical switches, see: Raymo, F. A.; Tomasulo, M. *Chem. Eur. J.* **2006**, *12*, 3186.

(2) To, T. T.; Barnes, C. E.; Burkey, T. J. *Organometallics* **2004**, *23*, 2708.

(3) To, T. T.; Duke, C. B., III; Ross, C. R; Barnes, C. E.; Webster, C. E.; Burkey, T. J. Preparation and Irradiation of $(C_5H_4R)Mn(CO)_3$ Derivatives with Chelatable Functional Groups: Studies of Linkage Isomerization as a Mechanism for Photochromic Materials. *Organometallics*, in preparation.

(4) These were the first examples of unit quantum yields for organometallic photosubstitution. For R = $C(O)CH_3$, where no chelate can form, the quantum yield is 0.82. Please see the following: Jiao, T.; Pang, Z.; Burkey, T. J.; Johnston, R. F.; Heimer, T. A.; Kleiman, V. D.; Heilweil, E. J. *J. Am. Chem. Soc.* **1999**, *121*, 4618.

(5) (a) Wiland, S.; van Eldik, R. *J. Phys. Chem.* **1990**, *94*, 5865. (b) Burdett, J. K.; Grzybowski, J. M.; Perutz, R. N.; Poliakoff, M.; Turner, J. J.; Turner, R. F. *Inorg. Chem.* **1978**, *17*, 147.

(6) (a) Lian, T.; Bromberg, S. E.; Asplund, M. C.; Yang, H.; Harris, C. B. *J. Phys. Chem.* **1996**, *100*, 11994. (b) Kim, S. K.; Pedersen, S.; Zewail, A. H. *Chem. Phys. Lett.* **1995**, *233*, 500. (c) Schwartz, B. J.; King, J. C.; Zhang, J. Z.; Harris, C. B. *Chem. Phys. Lett.* **1993**, *203*, 503.

(7) (a) To, T. T.; Burkey, T. J.; Heilweil, E. J. *J. Phys. Chem. A* **2006**, *110*, 10669. (b) Yeston, J. S.; To, T. T.; Burkey, T. J.; Heilweil, E. J. *J. Phys. Chem. B* **2004**, *108*, 4582.

(8) Barbero, M.; Cdamuro, S.; Degani, I.; Dughera, S.; Fochi, R. *J. Org. Chem.* **1995**, *60*, 6017.

(9) ^{1}H NMR (270 MHz, $CDCl_3$, 298 K): δ 2.15 (s, 3H, SCH_3), 3.84 (s, 2H, CH_2), 5.27 (m, 2H, C_6H_5), 5.65 (m, 1H, C_6H_5), 6.12 (m, 2H, C_6H_5).

(10) ^{1}H NMR (270 MHz, $CDCl_3$, 298 K): δ 2.11 (s, 6H, $2(SCH_3)$), 4.88 (m, 1H, CH), 5.25 (m, 2H, C_6H_5), 5.66 (m, 1H, C_6H_5), 6.16 (m, 2H, C_6H_5).

(11) ^{1}H NMR (270 MHz, $CDCl_3$, 298 K): δ 2.06 (s, 9H, $3(SCH_3)$), 5.18 (m, 2H, C_6H_5), 5.69 (m, 1H, C_6H_5), 6.80 (m, 2H, C_6H_5).

(12) Certain commercial equipment, instruments, or materials are identified in this paper in order to adequately specify the experimental procedure. In no case does such identification imply recommendation or endorsement by NIST, nor does it imply that the materials or equipment identified are necessarily the best available for the purpose.

(13) Mahaffy, C.; Pauson, P. L. *Inorg. Synth.* **1990**, *28*, 136.

(14) (a) Creavens, B. S.; George, M. W.; Ginsburg, A. G.; Hughes, C.; Kelly, J. M.; Long, C.; McGrath, K. M.; Pryce, M. T. *Organometallics* **1993**, *12*, 3127. (b) Walsh, E. F.; George, M. W.; Goff, S.; Nikiforov, S. M.; Popov, V. K.; Sun, X.-Z.; Poliakoff, M. *J. Phys. Chem.* **1996**, *100*, 19425−19429.

(15) A reviewer proposed that the changes at 1880 and 1188 cm^{-1} are consistent with chelate converting to solvate. This would be unlikely since after CO dissociates in solution, collisions with the solvent do not leave enough energy for a second ligand to dissociate,[16] and this would also be the case by the time the chelate forms.

(16) Rayner, D. M.; Ishikawa, Y.; Brown, C. E.; Hackett, P. A. *J. Chem. Phys.* **1991**, *94*, 5471.

(17) Ross, B. L.; Grasselli, J. G.; Ritchey, W. M.; Kaesz, H. D. *Inorg. Chem.* **1963**, *5*, 1023.